ACS APPLIED MATERIALS & INTERFACES

Research Article

www.acsami.org

Novel Chitosan-Functionalized Spherical Nanosilica Matrix As an Oral Sustained Drug Delivery System for Poorly Water-Soluble Drug Carvedilol

Lizhang Sun,[†] Yanzhu Wang,[†] Tongying Jiang,[†] Xin Zheng,[†] Jinghai Zhang,[‡] Jin Sun,[†] Changshan Sun,[†] and Siling Wang*[,†]

[†]Department of Pharmaceutics, Shenyang Pharmaceutical University, P.O. Box 32, Liaoning Province, Shenyang 110016, P.R. China.

[‡]Key laboratory of Pharmaceutical Biotechnology, School of Life Science and Bio-pharmaceutics, Shenyang Pharmaceutical University, Liaoning Province, Shenyang 110016, P.R. China

Supporting Information

ABSTRACT: A novel spherical nanosilica matrix (SNM) together with chitosan (CTS) encapsulated SNM (CTS-SNM) was developed in order to investigate the feasibility of using chitosan to regulate drug release rate from porous silica and obtain an oral sustained drug delivery system. To achieve this goal, we synthesized a spherical nanosilica matrix (SNM) and incorporated chitosan chains on the SNM surface. Solvent evaporation method was adopted to load the model drug carvedilol into SNM and CTS-SNM. The physicochemical properties of the drug carriers and drug-loaded composites were systematically studied using scanning electron microscopy (SEM), transmission electron microscopy (TEM), nitrogen adsorption, X-ray diffraction (XRD), differential scanning calorimetry (DSC), and thermogravimetric analysis (TGA). The structural changes in CTS-SNM in simulated gastrointestinal fluid as well as the relationships between swelling effect of chitosan and in vitro drug release behaviors were investigated. Pharmacokinetic and bioavailability aspects were also discussed. The results showed that the powerful dispersing effect of SNM and the blocking action due to the swelling of chitosan were the two main factors contributing to the sustained drug release behavior. The swelling effect of chitosan in an acidic environment together with the shrinking effect in a relatively alkaline environment allowed regulation of drug release behavior in simulated gastrointestinal fluid. An in vivo study showed that the bioavailability of CAR was improved 182% compared with that of the commercial capsule when SNM was used as the drug carrier. As for CAR-CTS-SNM, the T_{max} of CAR was delayed by about 3.4 h and the bioavailability was slightly increased in comparison with the commercial capsule. We believe that SNM and CTS-SNM developed in this study will help increase the use of polymers and inorganic materials in pharmaceutical applications and stimulate the design of oral drug delivery systems for immediate or sustained release of poorly water-soluble drugs.

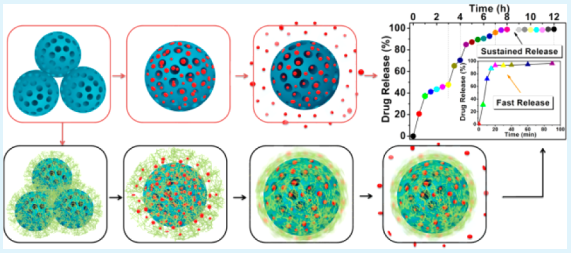

KEYWORDS: *nanosilica matrix, chitosan, drug delivery, sustained release, poorly water-soluble drug, carvedilol*

INTRODUCTION

Recent advances in nanotechnology have provided a variety of nanomatrix systems with highly controlled shapes and sizes, and a variety of interesting properties. These materials can prove useful in a variety of biomedical applications ranging from the diagnosis of diseases to the development of novel therapies.[1−3] In particular, because of the superior physical properties and ease of surface modification exhibited by silica, the discovery of mesoporous silica has been recognized as a milestone in materials science research and worldwide attention has been focused on using silica as an effective agent to improve the dissolution rate of poorly water-soluble drugs and/or regulate drug release by means of finely tuned surface functionalization.[4−6] To date, apart from the established series of nanosilica materials, like MCM or SBA-types, our research team have developed a number of new nanosilica matrices with a variety of morphologies and pore structures to be used in the pharmaceutical field, including spherical mesoporous silica nanoparticles, mesocellular foam silica nanoparticles and 3D ordered macroporous silica.[7−12] However, advanced drug delivery applications require more sophisticated drug carriers able to respond to biological or environmental stimuli and thus modulate drug release and adsorption characteristics.[13−15] Hence, a great deal of effort has been devoted to exploring novel drug vehicles with the aim of creating desired features to achieve so-called intelligent drug delivery such as targeted or sustained drug release systems.[16,17] In this context, how to combine the excellent properties of silica with the demand for advanced drug delivery systems has become a new topic of

Received: October 8, 2012
Accepted: December 13, 2012
Published: December 13, 2012

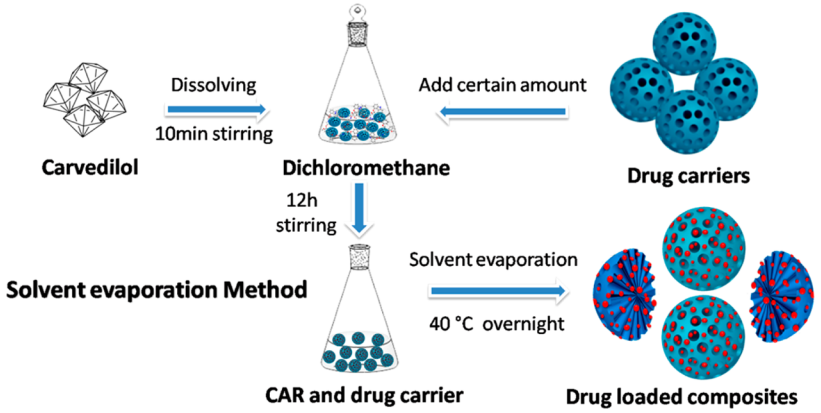

Figure 1. Schematic illustration of the drug loading procedure.

interest for all scientists working on the development of drug delivery systems.

As is well-known, a reduction in drug particle size can lead to an increased dissolution rate for many drugs and this strategy has been employed in the pharmaceutical industry for several decades.[18] Unlike the conventional preparation approach for nanoformulations where drug particles are stabilized with surfactants or polymers, mesoporous silica can retain the drug in a smaller space, ranging from 2 to 50 nm, and allow the drug to disperse efficiently in an amorphous or microcrystalline state. Meanwhile, the rigid porous structure of the silica provides a more stable environment for the nanoscale drug particles that are in a higher free energy state and with a greater molecular mobility. No doubt the technique of drug nanosizing using nanosilica will increase the drug stability and enhance the drug dissolution rate. Furthermore, the silanol groups scattered on the surface of the porous network allow easy chemical moiety modification or polymer coating and, therefore, allow functional modification of the silica to produce improved properties allowing the production of more advanced materials for many novel biological applications.[19,20] In general, surface modification of nanosilica can be carried out by either chemical or physical methods. Chemical interactions can lead to much stronger interaction between modifiers and silica nanoparticles, whereas surface modification based on physical interactions always takes place with the aid of hydrogen bonds or other interactions between the active groups on the modifier and the silanol groups on silica.[21,22] Among the widespread research into silica surface functionalization or modification, polymer coatings provide an alternative way of extending the properties of silica particles. As an important group of promising materials, biocompatible materials have attracted much attention for biomedical applications, such as the sustained release of drugs or macromolecules, pH-triggered drug release, and tissue targeted drug delivery.[23,24] However, few reports have been published on the application of a combination of the drug dispersing effect of silica with the retardant action of a polymer to control the release rate of poorly water-soluble drugs.

Here, we report for the first time the application of chitosan-grafted silica (CTS-SNM) as an effective drug carrier and discuss the feasibility of taking advantage of the dispersion effect of porous silica and the swelling properties of chitosan to control the drug release rate and achieve an oral sustained drug delivery system for poorly water-soluble drugs. To achieve this goal, we synthesized a spherical nanosilica matrix (SNM) with a spherical geometry. Chitosan chains were then introduced onto the silica surface through a postsynthetic method. Carvedilol, a well-known BCS II drug, was loaded into SNM and CTS-SNM using a classical solvent evaporation method. The physicochemical properties of the drug carriers and the drug-loaded composites were systematically studied using SEM, TEM, and nitrogen adsorption, XRD, low-temperature DSC, TGA, and UV spectrometry. The structural changes in the chitosan grafted silica over time in simulated gastrointestinal fluid along with the relationships between the swelling effect of chitosan and the in vitro drug release properties were systematically investigated. An in vivo study was conducted with SD rats and pharmacokinetic and bioavailability aspects are discussed in detail. We believe that the SNM and CTS-SNM developed in this study will help to expand the use of polymers and inorganic materials in the pharmaceutical field and the new information produced from our research will help promote the design of oral drug delivery systems for the immediate or sustained release of poorly water-soluble drugs.

EXPERIMENTAL SECTION

Materials. Tetraethyl orthosilicate (TEOS, GR), 1, 3, 5-triethylbenzene (TMB, AR), hexadecyl trimethyl ammonium bromide (CTAB, purity >99.0%) and ethyl ether (99.5%) were purchased from Aladdin (Shanghai, China). Anhydrous Ethanol (99.5%), dichloromethane (99.5%) and acetic acid (99.5%) were supplied by Shan Dong Yu Wang Reagent Company. Chitosan (DAC $\geq$ 95%) was obtained from Haidebei Biotechnology (Jinan, China). Commercial carvedilol capsules were produced by Southwest Synthetic Pharmaceutical Company. Raw carvedilol (purity >99.0%) was donated by Shenyang Funing Pharmaceutical Company (Shenyang, China). All the chemicals were used as received without any further purification. Deionized water was used in all experiments. Other chemicals were commercially available and used as-received.

Fabrication of Spherical Nanosilica Matrix. The SNM were synthesized by a facile process as reported by Xindu et al.[25] with some modifications. In a typical synthesis, a mixed solution was prepared in a 200 mL reaction vessel by dissolving 500 mg of CTAB in a mixture involving 70 mL of deionized water and 60 mL of ethanol. After a transparent solution was obtained, 0.6 mL of TMB was added to the surfactant solution. The suspension was stirred using a magnetic stirrer at 500 rpm for 30 min and then 1 mL of aqueous ammonia and 20 mL of ethyl ether were added dropwise to the solution to form a homogeneous emulsion. After vigorously stirring for 30 min at room temperature, 5 mL of TEOS was quickly dripped into the mixture, the reaction was preceded under agitation at 600 rpm for 4 h. The resulting white precipitate was further homogenized using an ATS AH100D homogenizer (ATS Engineer Inc., China) at 800 bar for 20 cycles to reduce the aggregation of nanoparticles. The obtained products were then filtered, sufficiently washed, and dried in air at 60

°C for 6 h. At last, all the organic components in the products were removed by calcination at 600 °C under atmospheric condition for 6 h.

Chitosan Encapsulation for CTS-SNM. Chitosan solution was obtained by dissolving 0.1 g of chitosan in 100 mL of 1.5 v/v % of acetic acid solution. The solution was stirred for 4 h at 600 rpm to dissolve chitosan completely. SNM solution with a concentration of 1 w/v % was prepared for subsequent use. For the encapsulation procedure, 5 mL of the 0.1 w/v % chitosan solution was added slowly, dropwise using a fine syringe, to an equal volume of 1 w/v % SNM under vortexing. The resultant mixture was then standing for 4 h to achieve a sufficient ionic attraction between chitosan and silica. Afterward, the solution thus obtained was then centrifuged at a speed of 6000 rpm and the residue was washed using deionized water. Centrifugation and washing were repeated for a total of five times. After the fifth round of centrifugation, the residue that would contain chitosan-encapsulated SNM was dried at 60 °C overnight. The obtained samples were crushed and passed through 80 mesh screen to give fine white powder.

Drug Impregnation into SNM and CTS-SNM. Carvedilol, a well-known BCS II drug, was selected as a model drug because of its poorly water-soluble and highly permeable nature. The drug impregnation process was performed as Figure 1 represented. First, 60 mg CAR was dissolved thoroughly in dichloromethane in a sealed vial (30 mg/mL), and then 150 mg of the fabricated porous silica was added into the solution to obtain samples with the drug/silica ratio of 1:2.5 (w/w). Afterward, the dispersion was ultrasonicated for a few minutes and gently stirred at ambient temperature (about 25 °C) for 12 h aiming at the maximum drug loading efficiency. Finally the solvent was allowed to evaporate under 45 °C for over 24 h in order to remove the solvent completely. The dried drug−silica composite named CAR-SNM was finally passed through an 80 mesh sieve, and stored in a vacuum dryer. The preparation process for CAR loading into CTS-SNM was similar to that used for loading CAR into SNM and the final product was named CAR-CTS-SNM.

FE-SEM and TEM Studies. The morphology and particle size of the prepared SNM and CTS-SNM were characterized using a field emission scanning electron microscope (JEOL-6700, Japan). All the samples were gold-coated under vacuum before examination. The porous structure of the samples was detected by a TecnaiG^2 F30 TEM instrument (FEI, The Netherlands). Prior to imaging, the obtained samples were dispersed in deionized water through sonication and then deposited on carbon-plated copper grids.

Nitrogen Adsorption Analysis. The information about surface areas and pore characteristics of the samples was obtained by determining the nitrogen adsorption isotherms using SA3100 surface area analyzer (Beckman coulter, USA). Prior to analysis, SNM samples were degassed under vacuum at 120 °C for 12 h, while the CTS-SNM and drug-loaded samples were degassed at 40 °C for 12 h. The surface areas were determined according to the Brunauer−Emmett−Teller (BET) method using experimental points at a relative pressure of P/P_0 = 0.05−0.25. The pore size distributions were calculated from the adsorption branch of N_2 isotherms by the Barrett−Joyner−Halenda (BJH) method. The total pore volume was estimated from the N_2 amount adsorbed at a relative pressure of 0.9814.

Drug Uptake Analysis by UV and TGA. The actual drug loading of CAR-SNM and CAR-CTS-SNM was ascertained by extracting an accurately weighed amount of CAR-loaded composites with methanol, followed by the determination of drug content using ultraviolet (UV) spectroscopy at a wavelength of 240 nm (UV-2000, Unico, USA). The standard curves were linear over the concentration range of 2.0−8.0 μg/mL. All measurements were carried out in triplicate. TGA-50 instrument (Shimadzu, Japan) was also employed to calculate the drug payload efficiency. A sample of about 3 mg was heated from 50 to 600 °C at a heating rate of 10 °C/min under N_2 purge of 20 mL/min. The drug loading content and entrapment efficiency were calculated by the ratio of the amount of CAR detected by UV to the amount of the CAR loaded composite and the initial amount of CAR, respectively.

Solid-State Characterization by PXRD and DSC. As the most powerful method, powder X-ray diffraction (PXRD) was used for the identification of the crystals (structure and changes) of the drug-loaded samples as well as the pure drug crystalline. As a complementary tool, differential scanning calorimetry (DSC) and low-temperature DSC were also adopted for characterization. The investigation was conducted using Rigaku Geigerflex powder X-ray diffractometer (Rigaku Denki, Japan), differential scanning calorimeter (DSC 60, Shimadzu Co., Japan) and low-temperature DSC (Mettler-Toledo, Switzerland), respectively. XRD patterns of the samples were collected over the 2θ angle range from 5 to 40° at a step size of 0.02° and a scanning rate of 4°/min. The DSC equipment was calibrated by indium and zinc. Under a nitrogen purge of 40 mL/min, samples were heated at 10 °C/min in aluminum pans. Low-temperature DSC were performed from 0 to 200 °C using a heating rate of 10 °C/min under a N_2 gas purge of 30 mL/min.

Equilibrium Concentration Study. The equilibrium concentration of different samples of CAR were measured in triplicate by adding excess amount of raw CAR, CAR-SNM and self-prepared amorphous CAR in 20 mL deionized water and phosphate buffer solution (pH1.2 and pH6.8). The mixture was kept in a shaking bed temperature incubator at 37 °C. At predetermined time intervals, 4 mL medium was extracted and filtered through a 0.22 μm membrane filter. The drug concentration was determined by UV centered at 240 nm.

In vitro Drug Release Study. The dissolution profiles of the raw drug and drug-loaded composite were studied by using a USP II paddle method with a dissolution apparatus (RC-8D, Tianjin Guoming Medical Equipment Co., Ltd.). All dissolution studies were carried out under sink conditions in triplicate. The CAR-SNM samples equivalent to 10 mg CAR were exposed to two different dissolution media (900 mL): enzyme-free simulated gastric fluid (SGF, pH1.2) and enzyme-free simulated intestinal fluid (SIF, pH6.8). The dissolution studies carried out for 90 min. In order to simulate the in vivo release characteristics, CAR-CTS-SNM composite equivalent to 10 mg CAR was exposed to three different release media (900 mL): enzyme-free simulated gastric fluid (pH1.2), enzyme-free simulated intestinal fluid (pH6.8) and enzyme-free phosphate buffer fluid (pH4.5) for 24 h. The drug dissolution and release studies were conducted at a constant temperature (37 °C) with a paddle speed of 100 ± 1 rpm. At appropriate sampling times, 5 mL aliquots were withdrawn and filtered through a 0.22 μm membrane filter and an equal amount of fresh dissolution medium was instantly added to maintain a constant dissolution volume. Ultraviolet spectrophotometry (UV-2000, Unico, USA) was used to determine the amount of carvedilol released at a detection wavelength of 240 nm according to the rules of Chinese Pharmacopeia 2010.

In vitro pH-Response Study. To integrally evaluate the drug release process from CTS-SNM in the body, we employ a dialysis bag method to mimic the CAR release profiles in the gastrointestinal tract. The experimental conditions were as follows. First, a dialysis bag loaded with 30 mg CAR-CTS-SNM was put into a beaker filled with 900 mL of pH 1.2 PBS and the system was maintained at 37 °C for 3 h with 150 rpm stirring. Then, the post-test sample was placed sequentially into 900 mL of pH 4.5, 6.8, and 7.4 PBS for 1 h, 3 and 6 h to study the release behaviors of CAR in duodenum, small intestine, and colon, respectively. The conditions for the latter were consistent with those mentioned above except for the stirring rate tailored to 50 rpm. At given time intervals, 5 mL of release medium was removed for analysis and the determination process followed the rules described in the in vitro drug release study section.

Swelling Characterization for Chitosan-Grafted Silica. Aim to describe the structure changes of chitosan in CTS-SNM during the gastrointestinal tract, the specific surface area and pore volume were studied using SA3100 surface area analyzer. Briefly, four pieces of dialysis bags were prepared and each one was loaded with certain amount blank CTS-SNM. The obtained four dialysis bags were placed together into a beaker filled with PBS solution. The specific operation bring into correspondence with that for drug release simulation test. At the end of each part of simulation, one of the dialysis bags was taken out and the content was dried at 40 °C. Then nitrogen adsorption analysis was carried out following the instructions for CTS-SNM as described in nitrogen adsorption analysis section.

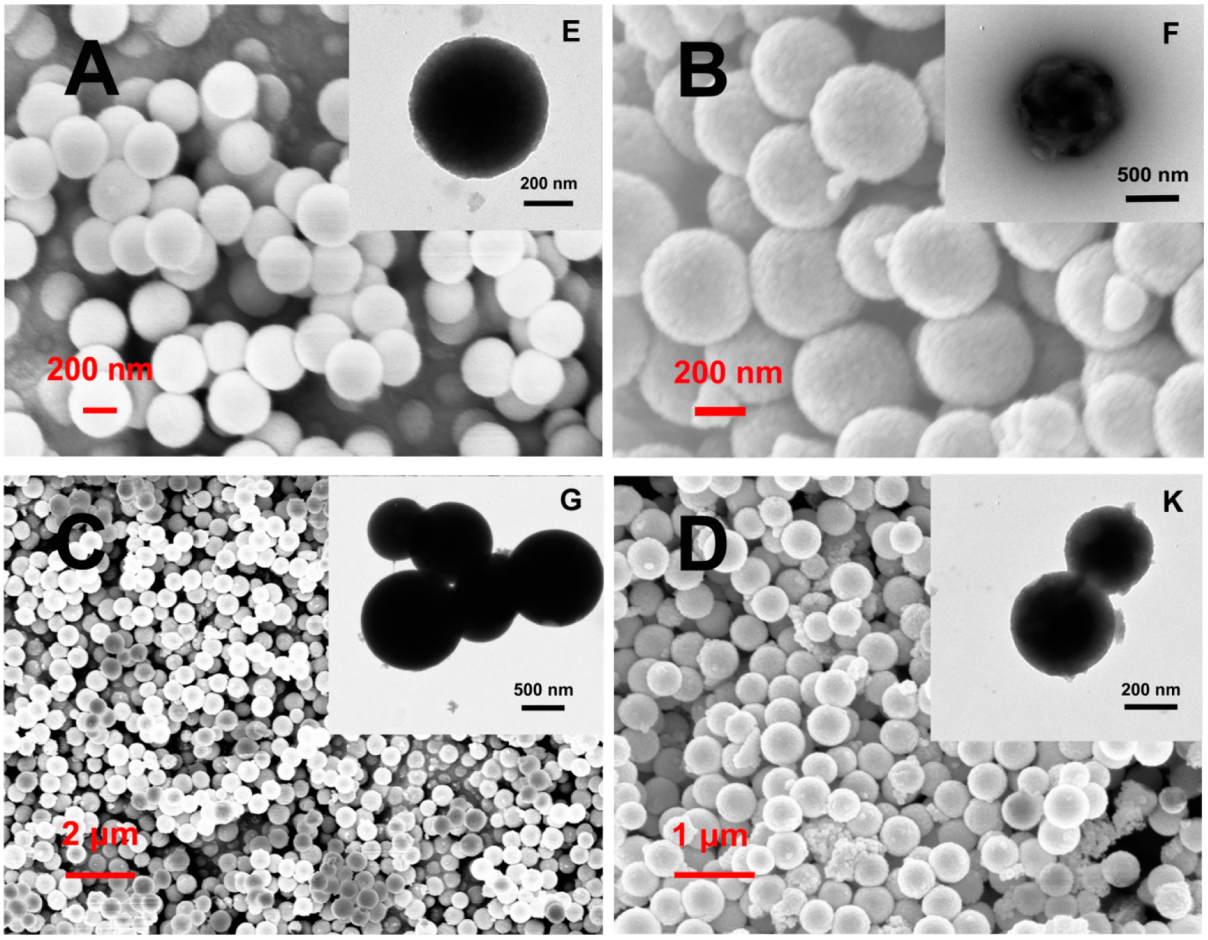

Figure 2. SEM and TEM micrographs of (A, E) SNM, (B, F) CTS-SNM, (C, G) CAR-SNM, (D, K) CAR-CTS-SNM, respectively.

In vivo Evaluation of CAR from SNM and CTS-SNM. The in vivo experiments were performed on male Sprague−Dawley rats (200 ± 20 g). All the animal experiments complied with the Animal Care and Use institutional guidelines and approval was granted by the Animal Ethics Committee of Shenyang Pharmaceutical University. Rats (n = 18) was divided evenly and randomly into 3 groups. Prior to experiments, they were fasted overnight and allowed free access to water. Commercial carvedilol capsule, self-prepared CAR-SNM and CAR-CTS-SNM suspensions were given by intragastric administration at a dose of 50 mg/kg. Blood samples (0.5 mL) were obtained from the eye socket vein before dosing and 15, 30, 45, 60, 90, 120, 240, 360, 480, 720, and 1440 min after dosing. Immediately after blood collection, centrifugation was conducted at 4000 rpm for 10 min and the given plasma was then transferred to a fresh Eppendorf tube (1.5 mL) and stored at −20 °C prior to analysis by HPLC. Plasma samples (200 μL) and internal standard β-naphthol (4 μL, 25.76 μg/mL) were mixed with NaOH (50 μL, 0.1 mol/L) and the mixture was vortexed for 3 min. After that, 1 mL of ethyl ether was added. The samples were vortexed for 5 min and the organic layer was separated by centrifugation at 10 000 rpm for 10 min. The supernatant was transferred to Eppendorf tubes (1.5 mL) and dried under nitrogen flow. The enrichment obtained was redissolved with Methanol (100 μL). The mixture was vortexed for 3 min and then centrifuged at 10000 rpm for 10 min. The supernatant was collected and 20 μL were injected into an HPLC for analysis [mobile phase methanol:acetonitrile:0.03 mol/L PBS (1:1:2), flow rate (1 mL/min)]. Over the range 0.04−4.0 μg/mL, the concentration of carvedilol was linearly proportional to the chromatographic peak area/internal standard area (correlation >0.99). The pharmacokinetic parameters were calculated using DAS 2.0 version (Mathematical Pharmacology Professional Committee of China).

RESULTS AND DISCUSSION

SNM were prepared by a cosolvent method coupled with a pore expanding process.[26] A typical swelling agent, TMB, was applied to prepare large pore SNM. In contrast to the traditional preparation method, the more simple procedure and moderate reaction conditions clearly shortened the synthesis time and are more suitable for industrial-scale production. The chitosan coating process was achieved by a postsynthesis approach. A great deal of research has been conducted on the zeta potential of silica and the results have shown that silica has a negative zeta potential under a wide range of pH conditions while the long-chain chitosan molecules are positively charged in the weak acid media so that adsorption can easily take place due to electrostatic attraction.[27] In addition, the large number of amino and hydroxyl groups on chitosan molecules will form more hydrogen bonds with the silanol groups on the silica surface and increase the binding between SNM and chitosan.

From the SEM micrographs (Figure 2A, B), we can see that the SNM and CTS-SNM produced both exhibit a non-aggregated spherical morphology and an average diameter of approximately 500 nm. Generally, the SEM images showed that the SNM encapsulated by chitosan are round in shape and the size of the CTS-SNM nanoparticles have slightly increased due to the chitosan encapsulation. The structure of SNM and CTS-SNM were further investigated by TEM. As illustrated by Figure 2E, F, pores, derived from CTAB and ethyl ether gasification, respectively, are present on the edge of the

particles. Especially for the SNM samples, the mesostructures are slitlike in shape and homogeneously distributed on the surface of the nanosphere. Following the modification of chitosan, the surface of CTS-SNM became uneven compared with the SNM samples. The results above confirmed the successful encapsulation of the silica nanoparticles by chitosan.

As shown in Figure 2C, D, the drug-loaded samples (CAR-SNM, CAR-CTS-SNM) retained an almost monodispersed spherical shape. Looking at the TEM images inset (Figure 2G, K), there were hardly any pores on the particle surface, indicating that most of the nanocavities of the drug carriers were filled with CAR. In addition, no CAR in crystalline form can be observed in the SEM images. This observation was in agreement with some previous research which demonstrated that drugs could be completely incorporated into the silica pores at suitable drug−silica ratios, or else crystals are formed from the redundant drug molecules.[9]

The actual drug loading content of the drug-carrier composites was quantified by TGA and UV spectrometry studies. The TGA curves for pure CAR, blank SNM, CTS-SNM, CAR-SNM, and CAR-CTS-SNM are all shown in Figure 3. The specific data for the drug loading content and entrapment efficiency determined by the two methods are listed in Table 1.

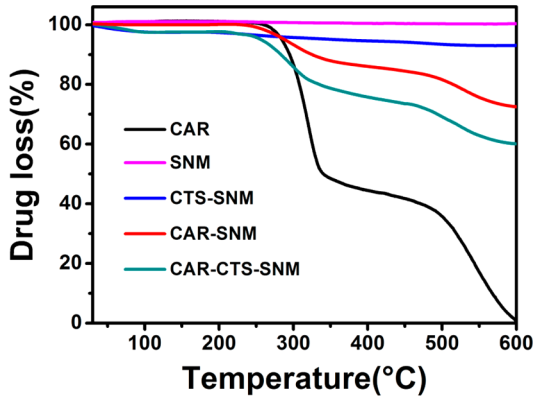

Figure 3. TGA patterns of CAR, SNM, CTS-SNM, CAR-SNM, and CAR-CTS-SNM.

With respect to the TGA analysis, the drug loading fractions were calculated from the ratio of the mass loss to the total initial mass between 20 and 600 °C. From the TGA patterns, it is clear that CAR had decomposed entirely by 600 °C, showing that is was a reliable method for estimating the drug loading efficiency. Because of the calcination step in the preparation process, almost a horizontal line was obtained for blank SNM, which suggested that no organic residues were present in the pure SNM. However, a clear mass loss of 6.95% for CTS-SNM was observed, which indicated the mass ratio of chitosan adsorbed in SNM to the overall CTS-SNM. Interestingly, the decline in the curve started from a low temperature of about 50 °C. This may be attributed to the evaporation of absorbed water tightly bound to the polymer.[28] The mass loss of CAR-SNM and CAR-CTS-SNM resulting from drug uptake was about 28.02 and 32.49%, respectively, which was consistent with the loading percentage obtained by UV spectrometric determination (as shown in Table 1). Surprisingly, despite having a smaller volume (as discussed in the nitrogen adsorption analysis below) than that of SNM, the chitosan modified drug carrier exhibited a higher drug loading efficiency. From the chemical structure differences between CAR and CTS, we can rationally speculate that the high drug loading efficiency of CTS-SNM was the result of interactions between the amino and hydroxyl groups on chitosan and two second amino and a hydroxyl groups on carvedilol. Furthermore, from the results of previous studies, which demonstrated that inorganic carriers tend to have a low encapsulation efficiency,[29] in our case, the drug loaded composite exhibited a high encapsulation efficiency (96.25% for SNM; 94.95% for CTS-SNM), which was very effective in maintaining the drug stability inside the carriers.

The nitrogen adsorption/desorption isotherms of SNM, CTS-SNM, CAR-SNM, CAR-CTS-SNM are presented in Figure 4. The data for the BET specific surface area (S_{BET}),

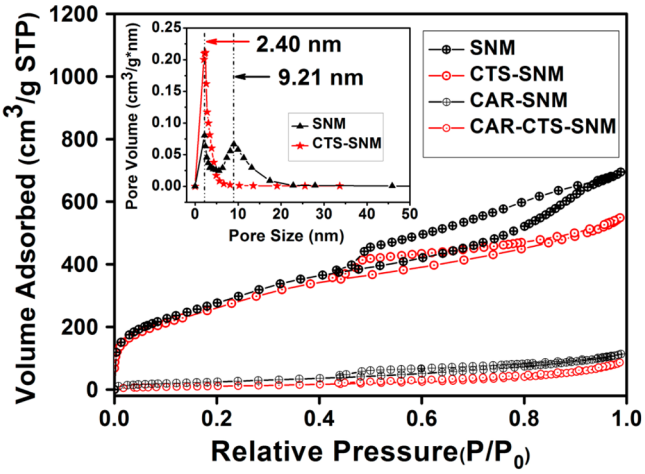

Figure 4. N_2 adsorption−desorption isotherms of SNM (black) and CTS-SNM (red) before and after drug loading. The inset shows the pore sizes distribution of SNM and CTS-SNM.

the total pore volume (V_t) and the pore diameter (D_p) are provided in Table 1. From the nitrogen adsorption/desorption isotherms, SNM and CTS-SNM both exhibited typical type IV features with type H4 hysteresis loops according to the IUPAC classification,[30] indicating a narrow slitlike pore structure. These results agreed well with those of the TEM observations.

Table 1. Properties Characterization for Drug Carriers before and after Drug Uptake

sample	D_p[a] (nm)	S_{BET}[b] (m^2/g)	V_t[c] (cm^3/g)	loading content (%,UV)	loading content (%,TGA)	entrapment efficient (%)
SNM	2.40; 9.21	1136.24	1.06			
CTS-SNM	2.40	635.14	0.63			
CAR-SNM		94.87	0.17	27.50 ± 0.89	28.02 ± 1.33	96.25 ± 3.12
CAR-CTS-SNM		42.28	0.13	31.65 ± 1.41	32.49 ± 1.57	94.95 ± 4.24

[a]D_p is the pore diameter calculated by BJH method on the branches of the nitrogen sorption isotherms. [b]S_{BET} is the BET surface area calculated using experimental points at relative pressure of P/P_0 = 0.05−0.25. [c]V_t is the total pore volume determined at the relative pressure of 0.98.

dx.doi.org/10.1021/am302246s | ACS Appl. Mater. Interfaces 2013, 5, 103−113

It can be seen from Table 1 that SNM and CTS-SNM samples both have a high S_{BET} and V_t, indicating their potential application as a host in bonding or storing drug molecules in the drug-release system. Furthermore, compared with SNM, samples after CTS modification exhibited reduced values of S_{BET} and V_P, confirming that the long-chain chitosan molecules are successfully attached to the SNM surface or porous structures. The reason for this phenomenon may be due to an electrostatic attraction between the negative silica and positive chitosan under the reaction conditions used, as described in the synthesis analysis. It was also clear that the shape of the hysteresis loop of CTS-SNM remained unchanged, suggesting that the pore shape was not significantly changed after the CTS wrapping process. The inset curves show the pore size distribution of SNM and CTS-SNM. It was clear that the SNM sample exhibits two intensive pore diameter peaks (2.40 and 9.21 nm) but, after CTS encapsulation, the pore size peak at 9.21 nm disappeared, indicating the strong effect of chitosan on pore blocking, although the pore volume of CTS-SNM was still large enough for drug loading. Table 1 also gives the data for SNM and CTS-SNM loaded with CAR. When CAR molecules were loaded, the total pore volumes of SNM and CTS-SNM were reduced from 1.06 to 0.17 cm^3/g and from 0.63 to 0.13 cm^3/g respectively. The sharp reduction in the adsorption capacity showed that a large number of CAR molecules had been loaded into the mesoporous channels. In addition, the drug loading process apparently altered the BET surface areas of SNM and CTS-SNM, which decreased from 1136.24 to 94.87 m^2/g for SNM and from 635.14 to 42.28 m^2/g for CTS-SNM, respectively. The results described above all demonstrate that CTS had been successfully introduced into SNM and the drug molecules were successfully loaded into the pores of SNM and CTS-SNM samples.

The state of CAR in the composite was evaluated by PXRD and DSC analysis. The PXRD and DSC patterns of SNM, CTS-SNM, drug-loaded samples, and the physical mixture are presented in Figures 5 and 6, respectively.

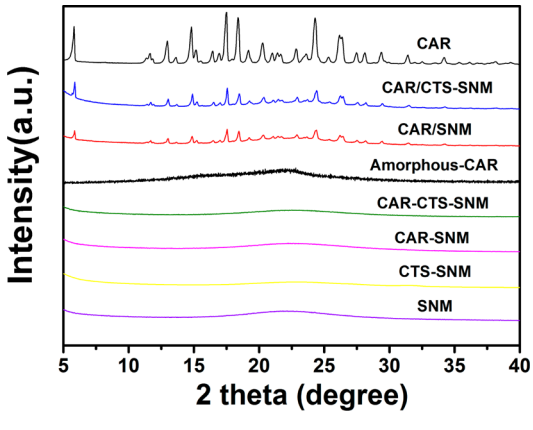

Figure 5. XRD patterns of CAR, SNM, CAR-SNM, CAR-CTS-SNM, and physical mixture (CAR/SNM, CAR/CTS-SNM).

As shown in Figure 5, the characteristic diffraction peaks for pure CAR at 5.7, 18.4, and 24.4° were particularly distinctive, indicating a highly crystalline state. Likewise, clear crystalline peaks attributed to pure CAR were also found for the physical mixture of drug and carrier mixed in the drug loading ratio, which implied that the drug carrier had no influence on the drug crystalline transition in a physically mixed condition. In

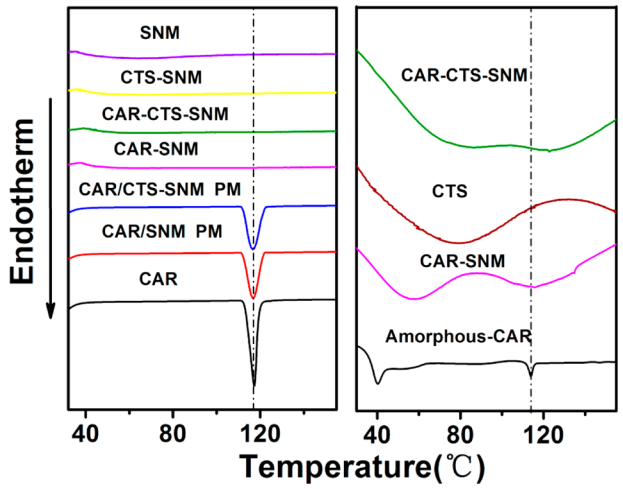

Figure 6. DSC thermogram (left) of CAR, SNM, CAR-SNM, CAR-CTS-SNM, physical mixture (CAR/SNM, CAR/CTS-SNM); low-temperature DSC thermogram (right) of CAR-SNM, CAR-CTS-SNM, CTS, and amorphous CAR.

contrast, due to the noncrystalline form of the blank SNM and CTS-SNM, no distinctive diffraction peaks were detected. In addition, amorphous CAR was successfully prepared by a typical melt quenching cooling approach and there were no distinct diffraction peaks shown in the PXRD patterns. Similarly, no crystalline peaks were shown for the drug-loaded samples suggesting that all drug absorbed in the pores or surface of the drug carriers was in an amorphous state. It is rational to suppose that the powerful dispersion effect of the nanocavities played an important role in the transformation of the drug from a crystalline state into a noncrystalline one.

The conventional DSC curves (left) for pure CAR, blank carriers, physical mixture and drug loaded composites together with the low-temperature DSC patterns (right) for CTS, CAR-SNM, CAR-CTS-SNM and amorphous CAR are all shown in Figure 6. The DSC thermogram of crystalline CAR exhibited a single sharp endothermic peak at 117.36 °C, which was in agreement with its intrinsic melting point.[31] Endothermic peaks for the physical mixture attributed to the melting of CAR are shown at 116.72 °C, indicating that SNM and CTS-SNM did not change the crystal structure of CAR. In comparison, no characteristic melting peak can be found in the DSC curves for the drug loaded samples. Considering the possibility of a masking effect of drug carriers on crystalline CAR, further studies were performed using low-temperature DSC analysis to further confirm the form of CAR present in the drug-carrier composites. It is known that amorphous substances aging at a temperature below the glass transition temperature (T_g) exhibit crystallization of the amorphous state via the equilibrium supercooled liquid state. The material experiences a gradual loss in terms of enthalpy because of the effect of the molecular motion occurring under the prevailing conditions, which drives the material toward a more stable crystalline state. This loss of enthalpy is recovered by the sample at Tg during its heating run in DSC and can be measured overtime.[32] Crystalline carvedilol has a melting point of about 117 °C and previous research has shown that the glass transition onset temperature of CAR is about 39.52 °C and the exothermal peak temperature is about 39 °C.[31] As shown in Figure 6 (right), the gradual slope for the prepared amorphous CAR is clearly seen around 35 °C, and the melting point peak has disappeared. This is a typical feature of

dx.doi.org/10.1021/am302246s | ACS Appl. Mater. Interfaces 2013, 5, 103−113

amorphous structures. For the CAR-SNM, the slope became more gradual and no endothermic peak was detected around 117 °C, which confirmed the amorphous form of CAR. Likewise, a similar curve was also observed for CAR-CTS-SNM. Apart from this, compared with the DSC patterns of CTS and CAR-SNM, the low temperature DSC curve of CAR-CTS-SNM is superposition of that of CTS and CAR-SNM. Together with the analysis of the PXRD, DSC and low-temperature DSC data, we believe that the drug confined to the nanocavities of SNM and CTS-SNM is in an amorphous state. Moreover, based on the experiments conducted previously, drug in an amorphous state can also be detected if the carrier/drug ratio is above 1:2. The most plausible explanation of this phenomenon is the very marked dispersion effect of the porous drug carrier.

The study conducted above provides strong evidence to explain the drug dissolution enhancement and provides a parallel platform for the subsequent comparative study to demonstrate the effect of chitosan on the regulation of the drug release rate. Besides, in order to investigate the stability of the carvedilol amorphous state in the formulations under standard storage conditions, accelerated stability test was carried out and the results indicated that all the criteria were in line with the quality standard specification after accelerated stability test for 3 months(Table 1, 2 and Figure 1, 2 in Supporting Information). The samples are still being tested for a longer storage period.

The equilibrium concentrations of pure CAR, amorphous CAR and CAR-SNM in different media were evaluated in order to demonstrate the powerful effect of SNM on drug dispersion and emphasize the influential role that SNM plays in improving the dissolution rate of poorly water-soluble drugs. This study provides a foundation for research into the swelling and retardant effects of chitosan on regulation of the drug release rate.

As shown in Figure 7, because of the alkaline nature of CAR, the results for all the samples displayed a significant pH-dependence. The experimental data indicated that the raw CAR possesses a very low solubility in water (23.58 ± 1.93 μg/mL) and pH 6.8 PBS (28.54 ± 3.92 μg/mL), which is consistent with a literature report[33] and a significant increase was observed in pH 1.2 medium (96.57 ± 5.35 μg/mL). The equilibrium concentration of amorphous CAR was increased 2-fold compared with the raw CAR, which was in agreement with the published literature showing that the prepared amorphous carvedilol failed to exhibit improved solubility.[34] The explanation for this was the conversion of the amorphous drug to a cohesive supercooled liquid at 37 °C, which is a temperature close to the glass transition temperature of amorphous carvedilol. Therefore, the equilibrium concentration did not increase markedly as expected. However, after drug nanosizing by SNM, the equilibrium concentrations of CAR-SNM in all the experimental media were almost four times higher than those of raw CAR (more specific data can be found in Table 3 in the Supporting Information), which strongly confirms the excellent ability of SNM to disperse the drug molecules and reduce the drug particle size.

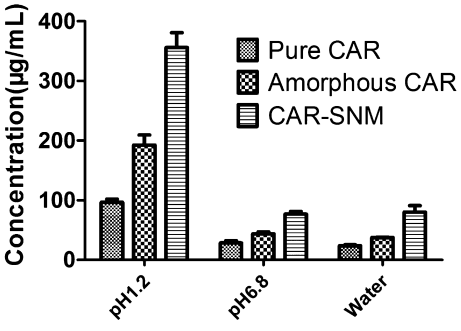

Figure 7. Equilibrium concentrations of CAR, amorphous CAR, and CAR-SNM in different media.

The in vitro study was carried out in enzyme-free simulated gastric fluid (pH1.2), intestinal fluid (pH6.8) and enzyme-free phosphate buffer (pH4.5) dissolution medium. The dissolution profiles of pure crystalline CAR as well as the CAR release profiles from CAR-SNM and CAR-CTS-SNM are all presented in Figure 8.

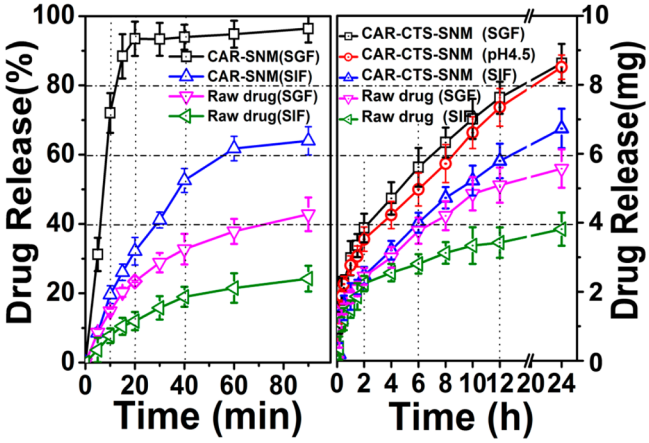

Figure 8. Dissolution and release profiles of CAR from CAR-SNM (left) and CAR-CTS-SNM (right) in different dissolution media. Each data point represents the mean ± SD of three determinations.

Because of its weakly basic nature, CAR exhibits a pH-dependent solubility. On the whole, the observed dissolution rates increased with the decrease in the pH values of the dissolution media. As is shown in Figure 8 (left), the dissolution of CAR from CAR-SNM was very fast in the simulated gastric fluid and reached 72.04% after 10 min and the amount of CAR dissolving from SNM within 40 min reached 93.91%, which complied well with the requirements of the Chinese Pharmacopoeia 2010 for commercial CAR products. However, in the simulated intestinal fluid, the drug dissolution rate fell markedly, but was a great improvement compared with that of the raw drug. The amounts of dissolved CAR in the simulated intestinal fluid at sampling times of 10, 20, and 40 min reached 19.61%, 32.15 and 52.56% for CAR-SNM. The corresponding amounts were 7.76, 11.99, and 18.98% for raw CAR. This improved dissolution may be largely attributed to the marked dispersing effect of the pores of SNM transforming the crystalline state of CAR into a noncrystalline state, which is well-known to improve the drug dissolution rate.

Figure 8 (right) shows a typical sustained release pattern of CAR from the CTS-modified SNM in SGF release medium. Remarkably, a burst release occurred in the initial 2 h and nearly 40% of the CAR was released into the SGF release medium. This is very useful for immediate drug therapy. Then, a slow and even release pattern was observed over a time period of about 24 h. The amount of released CAR at the sampling time of 6 h reached 56% and almost 80% of CAR dissolved

dx.doi.org/10.1021/am302246s | ACS Appl. Mater. Interfaces 2013, 5, 103−113

within 12 h. The reason for this may be that when the drug-carrier composites were dispersed in the release medium, the CAR molecules adsorbed on the surface of the drug carriers were initially moistened, which allowed increased diffusion for drug release. Therefore, it is easy to understand that in the early stage of drug release, the release rate of the loaded CAR was much faster than that of raw CAR. At the same time, the drug present in the pores of CTS-SNM was gradually released into the release medium, but needed to go through the blocking membrane formed by the swelling chitosan. Thus, the rest followed a typical sustained release pattern. Similar to the dissolution tendency for CAR from CAR-SNM, an acid medium seems to be more favorable for drug release than a neutral medium. Furthermore, the kinetics of the drug release in SGF and SIF examined by the Higuchi model showed a good linear fit between the fractional release of CAR (f_{CAR}) versus the square root of the release time (h) (see Tables 4 and 5 in the Supporting Information), indicating that the release of the drug from the pores of SNM and CTS-SNM is basically a diffusion process. In SGF release media, for CAR-CTS-SNM, $f_{CAR} = 18.08t^{1/2}$; for CAR-SNM, $f_{CAR} = 9.74t^{1/2}$. In the SIF release media, for CAR-CTS-SNM, $f_{CAR} = 14.76t^{1/2}$; for CAR-SNM, $f_{CAR} = 7.71t^{1/2}$.

Combined with the dissolution and release profiles of CAR from SNM and CTS-SNM in various dissolution media, it is evident that the strong dispersing effect of SNM markedly improved the drug dissolution rate but, under the same conditions of drug dispersing, the release rate of CAR from CAR-CTS-SNM was markedly retarded. The differences in release rate could be largely attributed to the CTS grafted on the pores and surface of SNM. It is predictable that the SNM and CTS-SNM prepared in our study could stimulate new ideas about the design of oral sustained drug delivery systems for poorly water-soluble drugs.

To thoroughly investigate the release rates of CAR from CAR-CTS-SNM and explore the relationships between the drug release behaviors and the swelling effect of chitosan, we employed a series of PBS solutions with pH values ranging from 1.2 to 7.4 to simulate the drug release along the gastrointestinal tract.

Figure 9 shows the S_{BET} and V_P changes for CTS-SNM at various pH values. In general, along with the increase in pH, the S_{BET} and V_P both displayed trend to decrease. Specifically, a

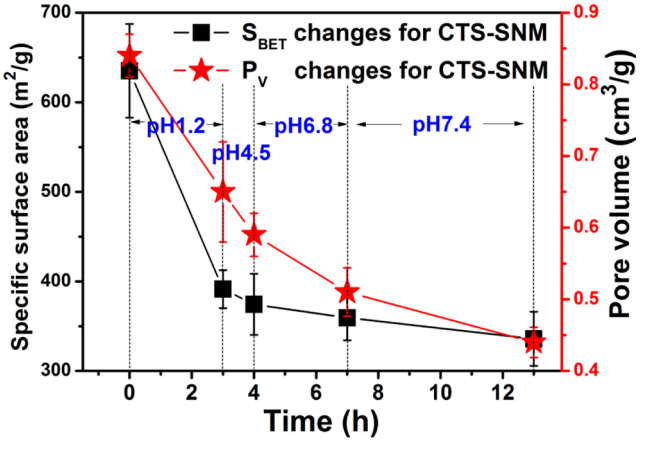

Figure 9. Specific surface area and pore volume changes at different sampling times in simulated gastrointestinal fluid for CTS-SNM (n = 3).

significant decrease in the S_{BET} of CTS-SNM occurred during the first 3 h. Over this time period, chitosan chains wrapped on the surface of SNM swelled in acid solution, leading to blockage of the nanocavities and a decline in S_{BET} and V_P. Interestingly, almost no changes in S_{BET} were observed after the first 3 h. Two factors may account for this result. (i) Chitosan chains were distributed on the surface and it is possible to use not only CTS-SNM but also complexes of CTS and SNM to describe the state of the drug carriers. The swollen shell would make this state relatively stable. (ii) It is known that erosion always occurred along with the swelling action of chitosan, especially in an acid environment. The fragments resulting from the erosion effect continuously fill the pores of the drug carriers and a balance was obtained between the fragments inside and the outside solution. This will ensure the stability of S_{BET}. The continuous decline in the pore volume also confirms this.

The experiment involving drug release of CAR from CAR-CTS-SNM was performed under identical conditions and the changes in V_P and S_{BET} were also measured. As show in Figure 10, we can clearly see that at the end of the first 3 h in the SGF

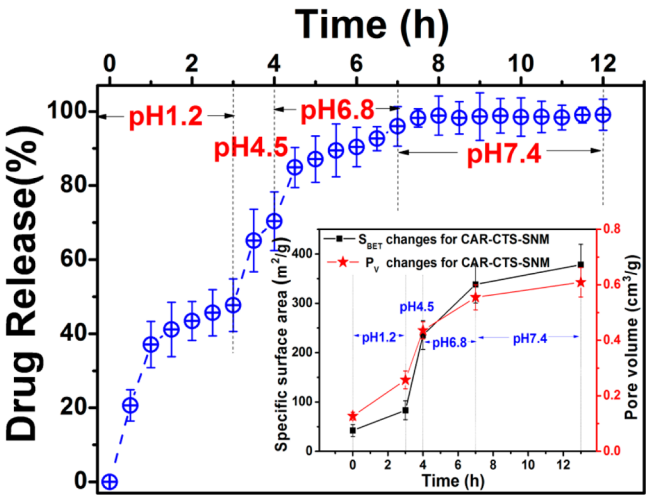

Figure 10. In vitro pH-response release behaviors of CAR from CAR-CTS-SNM in the release media of different pH values, which we used to simulate the conditions all through the gastrointestinal environment. Each data point represents the mean ± SD of three determinations. The inset is the specific surface area and pore volume changes at different sampling times in simulated gastrointestinal fluid for CAR-CTS-SNM (n = 3).

environment, the dissolved drug accumulated to about 40% and complete release of CAR from the CAR-CTS-SNM was observed within 12 h. This data was consistent with our former findings as discussed in the in vitro drug release section. Following conventional thinking, the V_P and the S_{BET} should exhibit a sharp increase with the constant release of CAR from the nanocavities. However, the increase in V_P and S_{BET} were not as clear as expected (Figure 10 inset). We have specifically discussed that at the beginning of the drug release process, the release of CAR was mainly dominated by the drug adsorbed on the CTS-SNM surface or mixed with chitosan and the release of the drug inside the pores was limited. On the other hand, the protective shell of the swelled chitosan also played a role in blocking the release of drug. Therefore, S_{BET} and V_P did not exhibit a significant increase within the first 3 h. It is known that the swelling effect is triggered by the protonation of the amino groups of chitosan at low pH values. This leads to repulsion in

dx.doi.org/10.1021/am302246s | ACS Appl. Mater. Interfaces 2013, 5, 103−113

the polymer chains and allows water to enter the gel network. Nevertheless, when the pH increased, amino groups become deprotonated, and repulsion in the polymer chains was reduced, allowing shrinkage. It is worth noting that the swelling ratio for chitosan did not produce any change until pH 4.0 but decreased drastically above pH 4.0, something which has been documented in other research.[35] In our case, when the complex was immersed in pH 4.5 medium, shrinkage may take place on the swelling shell. In such circumstances, the pores of CTS-SNM are exposed and a burst of drug release was observed at 5 h. Meanwhile, an apparent increase in S_{BET} and V_P was also observed, which further supported the shrinkage effect stated above. In addition, a similar burst release was recorded at 6 h when the release conditions switched to pH 6.8. This identical phenomenon further confirmed that the shrinkage of chitosan clearly affected the drug release behavior. Finally, the drug release became slower and the changes in S_{BET} and P_V tended to be very small.

It is worth noting that chitosan has a hydrophilic nature and it can improve the wetting effect for hydrophobic drug in gastrointestinal tract and thus, increase the drug release rate, which can be proved by the burst release effect. Interestingly, the release rate did not increase all the time and it slowed down obviously with a sustained release manner in the latter period. In addition, although chitosan and carvedilol are two different species, there are attractions between them, which we have mentioned in the discussion section on drug uptake analysis. The interaction was also a factor for the decrease in the drug release rate. But compared to the influence of the strong swelling effect of chitosan, the interaction between chitosan and carvedilol to drug release was so weak that it can be considered to be negligible in effect. Collectively, the interracial properties of chitosan and carvedilol indeed have an impact on the drug release pattern but cannot be established as the dominant factor. Furthermore, sustained release pattern was mainly affected by the swelling changes of chitosan all along the gastrointestinal tract.

It should also be noted that the environmental changes in vivo were not as dramatic as those under experimental conditions. Therefore, limitations still exist in the hypothetical mechanism we have elaborated above. Nevertheless, this study does suggest that there is a clear relationship between the properties of chitosan and the drug release behavior.

The in vivo study was conducted in order to investigate whether the rapid dissolution of CAR in vitro can be translated into an increased bioavailability and, furthermore, to explore whether the swelling properties of chitosan could alter the drug release behavior of CAR in vivo. Three different formulations were assessed: a commercial capsule, self-prepared CAR-SNM, and CAR-CTS-SNM. The plasma concentrations versus time profiles are presented in Figure 11 and the pharmacokinetic parameters are listed in Table 2.

As shown in Figure 11, when CAR was formulated in CAR-SNM, the C_{max} and AUC_{0-48h} after intragastric administration were increased nearly 2-fold compared with the commercial capsule. The C_{max} values for CAR-SNM and the commercial CAR capsule were 2.016 ± 0.368 and 1.041 ± 0.202 mg/L, respectively. The AUC_{0-48h} value for CAR-SNM was increased about 1.8-fold compared with that of the commercial CAR capsule. So, clearly, the self-prepared SNM drug carrier significantly improved the in vivo adsorption of carvedilol. In addition, the mean T_{max} for CAR-SNM was 1.667 h, representing a reduction of approximately one hour in

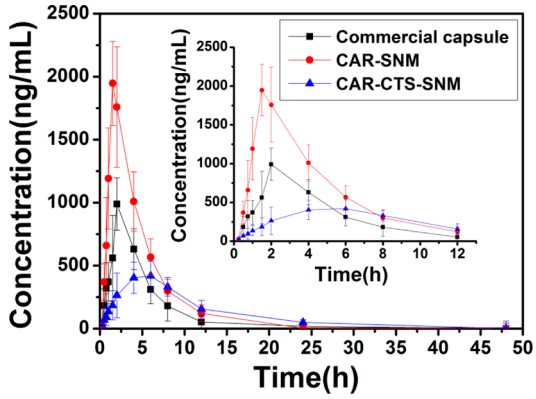

Figure 11. Plasma concentration−time profiles of carvedilol after intragastric administration of the carvedilol commercial capsule and drug-carrier composite in rats. Results are expressed as the mean with the bar showing SD values of six experiments.

Table 2. Pharmacokinetic Parameters of Commercial Capsule, Self-Prepared CAR-SNM, and CAR-CTS-SNM (100 mg/kg) after Intragastric Administration in Rats, mean ± S.D., n = 6

parameter	commercial capsule	CAR-SNM	CAR-CTS-SNM
$AUC_{(0-48)}$ (mg·h/L)[a]	4.986 ± 1.034	9.088 ± 1.516	5.272 ± 0.900
C_{max} (mg/L)[b]	1.041 ± 0.202	2.016 ± 0.368	0.460 ± 0.064
T_{max} (h)[c]	2.250 ± 0.880	1.667 ± 0.258	5.667 ± 1.506
MRT(h)[d]	6.072 ± 1.77	4.950 ± 0.835	10.259 ± 1.633
$t_{1/2}$(h)[e]	4.313 ± 1.312	4.226 ± 1.192	4.928 ± 0.471

[a]Area under the plasma concentration−time curve. [b]Maximum plasma concentration. [c]Time to reach C_{max}. [d]Mean residence time. [e]Elimination half-life.

comparison with the commercial CAR capsule, a result which would lead to increased drug effectiveness. The data listed above support the outstanding ability of SNM to enhance the oral bioavailability of carvedilol.

Interestingly, after intragastric administration of an equal amount of CAR-CTS-SNM, the T_{max} was delayed by about 3.4 and 4.0 h compared with the commercial capsule and self-prepared CAR-SNM, respectively. This agreed with the controlled-release formulation of CAR developed by other research groups.[36] The results obtained show that chitosan wrapped around the SNM results in an apparently limited drug release. However, the bioavailability of an equal amount of CAR-CTS-SNM was not significantly increased compared with the commercial capsule. On the contrary, the AUC_{0-48h} for CAR-CTS-SNM was actually 42% less than that of CAR-SNM. The reason for the poor bioavailability of CAR-CTS-SNM may involve two factors: first, carvedilol is extensively metabolized, mainly by conjugation with glucuronic acid and sulfuric acid and also by oxidation at different sites of the molecule. The quantity of drug released from CAR-CTS-SNM per unit time was much less than that from the immediate-release preparation and, thus, the chance of exposure to various potentially combinative substances was increased. This is bound to lead to extensive drug metabolism. Second, metabolism also occurs during the first passage through the liver after oral administration. Because of the saturability of the metabolic enzymes and the slow release features of the sustained-release formulation, the possibility of saturation of the metabolic

dx.doi.org/10.1021/am302246s | ACS Appl. Mater. Interfaces 2013, 5, 103−113

enzymes is reduced, and yet the possibility of metabolism of the released drug increases. Moreover, the protective effect and the nondegradable nature of the drug carrier may make the drug release behavior in vivo not as effective as that in vitro, and this may also contribute to the difficulty in improving bioavailability.

CONCLUSIONS

A novel chitosan-grafted spherical nanosilica matrix (CTS-SNM) has been developed in order to examine the feasibility of using biocompatible chitosan to regulate the drug release of carvedilol from the silica nanocavities. From the experimental results obtained, we have found that SNM alone can significantly increase the dissolution rate of the poorly water-soluble drug, carvedilol. This may be due to a transition of the drug from a crystalline state to an amorphous one, while the drug release rate from CTS-SNM was obviously controlled and met the requirements of the Chinese Pharmacopeia 2010 edition for a controlled drug release formulation. To explain the retardant effect of chitosan in detail, we systematically investigated the structural changes of chitosan in CTS-SNM at different times in simulated gastrointestinal fluid and explored the relationships between the swelling effect of chitosan and the drug release behavior. The results obtained showed that, after the burst release of drug adsorbed on the CTS-SNM surface or mixed with the chitosan shell, the release pattern of CAR from the CAR-CTS-SNM pores took place in pulses with a rise in pH all along the gastrointestinal tract, dominated by the swelling effect of chitosan under acidic conditions and the shrinking effect of a relatively alkaline environment. In addition, the in vivo study demonstrated that, after intragastric administration of CAR-CTS-SNM, the T_{max} was delayed by about 3.4 and 4.0 h relative to the commercial capsule and self-prepared CAR-SNM, respectively, which further confirmed the benefit of using chitosan for sustained drug delivery. Moreover, the high degree of drug metabolism and increased first-pass effect conspired to reduce the bioavailability of CAR-CTS-SNM.

Compared with the materials described in the literature, the drug release performance of this novel drug-loaded carrier presents the following features and advantages. First, as an orally administered drug carrier, it can significantly slow down the drug release rate, which has a positive meaning for frequency reduction in dosing and enhance convenience and compliance. Second, the release manner showed a pH dependency and this is of great practical value for drug targeting, especially for targeting release in the gastrointestinal tract. Third, the drug release rate is mainly dominated by silica dispersion and the chitosan swelling effect, and it satisfies the demand for wide range of drug types, which indicates extensive applications.

The chitosan functionalized spherical nanosilica matrix developed in our study combined the nanodispersion effect of porous silica and the retardant action of biocompatible chitosan and provided a new option for the sustained delivery of poorly water-soluble drugs. We believe that this novel drug carrier will encourage the use of polymers and inorganic materials in the pharmaceutical field and promote the design of oral drug delivery systems for immediate or sustained release of poorly water-soluble drugs.

ASSOCIATED CONTENT

Supporting Information

Detailed method for preparation of dissolution media, Method, results and discussion for accelerated stability test, Stability of CAR-SNM and CAR-CTS-SNM capsules in accelerated test, Equilibrium concentrations of CAR, amorphous CAR and CAR-SNM in different media, kinetics equations fitting by release data of CAR- SNM and CAR-CTS-SNM, XRD patterns and drug dissolution profiles for accelerate stability test. This material is available free of charge via the Internet at http://pubs.acs.org/.

AUTHOR INFORMATION

Corresponding Author

*E-mail: silingwang@syphu.edu.cn. Tel.: +86 24 23986346. Fax: +86 24 23986346.

Notes

The authors declare no competing financial interest.

ACKNOWLEDGMENTS

This work was supported by National Basic Research Program of China (973 Program) (2009CB930300), National Natural Science Foundation of China (81072605), Key Laboratory of Drug Preparation Design & Evaluation of Liaoning Provincial Education Department (LS2010161), Major national platform for innovative pharmaceuticals (2009ZX09301-012) and Shenyang Special Fund for Exploration of Intellectual Resources.

ABBREVIATIONS

SNM, spherical nanosilica matrix; CTS, chitosan; CAR, carvedilol; CTS-SNM, SNM was functionalized with chitosan; CAR-SNM, CAR-loaded SNM; CAR-CTS-SNM, CAR-loaded CTS-SNM

REFERENCES

(1) Hughes, G. A. *Nanomed. Nanotechnol. Biol. Med.* **2005**, *1*, 22−30.
(2) Vallet-Regí, M.; Balas, F.; Arcos, D. *Angew. Chem., Int. Ed.* **2007**, *46*, 7548−7558.
(3) Parveen, S.; Misra, R.; Sahoo, S. K. *Nanomed. Nanotechnol. Biol. Med.* **2012**, *8*, 147−166.
(4) Slowing, I. I.; Vivero-Escoto, J. L.; Wu, C. W.; Lin, V. S. Y. *Adv. Drug Delivery Rev.* **2008**, *60*, 1278−1288.
(5) Anglin, E. J.; Cheng, L.; Freeman, W. R.; Sailor, M. J. *Adv. Drug Delivery Rev.* **2008**, *60*, 1266−1277.
(6) Wang, S. *Microporous Mesoporous Mater.* **2009**, *117*, 1−9.
(7) Zhang, Y.; Jiang, T.; Zhang, Q.; Wang, S. *Eur. J. Pharm. Biopharm.* **2010**, *76*, 17−23.
(8) Du, X.; He, J. *Nanoscale* **2011**, *3*, 3984−4002.
(9) Hu, Y.; Zhi, Z.; Wang, T.; Jiang, T.; Wang, S. *Eur. J. Pharm. Biopharm.* **2011**, *79*, 544−551.
(10) Zhang, Y.; Zhang, J.; Jiang, T.; Wang, S. *Int. J. Pharm.* **2011**, *410*, 118−124.
(11) Hu, Y.; Wang, J.; Zhi, Z.; Jiang, T.; Wang, S. *J. Colloid Interface Sci.* **2011**, *363*, 410−417.
(12) Zhang, Y.; Wang, J.; Bai, X.; Jiang, T.; Zhang, Q.; Wang, S. *Mol. Pharm.* **2012**, *9*, 505−513.
(13) Mout, R.; Moyano, D. F.; Rana, S.; Rotello, V. M. *Chem. Soc. Rev.* **2012**, *41*, 2539−2544.
(14) Manzano, M.; Vallet-Regí, M. *J. Mater. Chem.* **2010**, *20*, 5593−5604.
(15) Arruebo, M. *Wires Nanomed. Nanobiol.* **2012**, *4*, 16−30.
(16) Ganta, S.; Devalapally, H.; Shahiwala, A.; Amiji, M. *J. Controlled Release* **2008**, *126*, 187−204.

(17) Rosenholm, J. M.; Sahlgren, C.; Lindén, M. *Nanoscale* **2010**, *2*, 1870−1883.
(18) Kesisoglou, F.; Panmai, S.; Wu, Y. *Adv. Drug Delivery Rev.* **2007**, *59*, 631−644.
(19) Lou, X.; Schumacher, T.; Yang, H.; Ding, A. *J. Controlled Release* **2011**, *152* (Suppl 1), e65−67.
(20) Jain, T. K.; Roy, I.; De, T. K.; Maitra, A. *J. Am. Chem. Soc.* **1998**, *120*, 11092−11095.
(21) Zou, H.; Wu, S.; Shen, J. *Chem. Rev.* **2008**, *108*, 3893−3957.
(22) Barbé, C.; Bartlett, J.; Kong, L.; Finnie, K.; Lin, H. Q.; Larkin, M.; Calleja, S.; Bush, A.; Calleja, G. *Adv. Mater. (Weinheim, Ger.)* **2004**, *16*, 1959−1966.
(23) Uhrich, K. E.; Cannizzaro, S. M.; Langer, R. S.; Shakesheff, K. M. *Chem. Rev.* **1999**, *99*, 3181−3198.
(24) Pillai, O.; Panchagnula, R. *Curr. Opin. Chem Biol.* **2001**, *5*, 447−451.
(25) Du, X.; He, J. *Langmuir* **2010**, *26*, 10057−10062.
(26) Boissière, C.; Martines, M. A. U.; Tokumoto, M.; Larbot, A.; Prouzet, E. *Chem. Mater.* **2003**, *15*, 509−515.
(27) Lvov, Y.; Ariga, K.; Onda, M.; Ichinose, I.; Kunitake, T. *Langmuir* **1997**, *13*, 6195−6203.
(28) López, F.; Mercê, A. L. R.; Alguacil, F. J.; López-Delgado, A. *J. Therm. Anal. Calorim.* **2008**, *91*, 633−639.
(29) Matsumura, Y.; Maeda, H. *Cancer Res.* **1986**, *46*, 6387−6392.
(30) Everett, D.; Haul, R.; Moscou, L.; Pierotti, R.; Rouquerol, J.; Siemieniewska, T. *Pure Appl. Chem.* **1985**, *57*, 603−619.
(31) Pokharkar, V. B.; Mandpe, L. P.; Padamwar, M. N.; Ambike, A. A.; Mahadik, K. R.; Paradkar, A. *Powder Technol.* **2006**, *167*, 20−25.
(32) Shamblin, S. L.; Zografi, G. *Pharm. Res.* **1998**, *15*, 1828−1834.
(33) Brook, C. S.; Chen, W.; Dell'Orco, P. C.; Katrincic, L. M.; Louvet, A. M.; Oh, C. K.; Spoors, P. G.; Werner, C. *Carvedilol phosphate salts and/or solvates thereof, corresponding compositions, and/or methods of treatment*. U.S. Patent 7 268 156, Sept 11, 2007.
(34) Planinšek, O.; Kovačič, B.; Vrečer, F. *Int. J. Pharm.* **2011**, *406*, 41−48.
(35) Rohindra, D. R.; Nand, A. V.; Khurma, J. R. *J. Nat. Appl. Sci.* **2004**, *22*, 32−35.
(36) Fonarow, G. C. *Expert Opin. Pharmacother.* **2006**, *7*, 2533−2546.